Double Isocyanide Insertion and C,C-Coupling Reaction of $[(C_5Me_4)SiMe_2(N\text{-}t\text{-}Bu)]ZrMe_2$. Structural Characterization of the Two 1,4-Diaza-5-zirconacyclopentene Ring Conformations for $[(C_5Me_4)SiMe_2(N\text{-}t\text{-}Bu)]Zr[N(R)C(Me)=C(Me)N(R)]$ Complexes

Lioba Kloppenburg and Jeffrey L. Petersen*

Department of Chemistry, West Virginia University, Morgantown, West Virginia 26506-6045

Received December 18, 1996[⊗]

The reactions of 2 equiv of CNR (R = (**a**) *tert*-butyl, (**b**) 2,6-xylyl, (**c**) Me) with $[(C_5Me_4)SiMe_2(N\text{-}t\text{-}Bu)]ZrMe_2$, **1**, proceed sequentially with isocyanide insertion into both Zr−C(methyl) bonds of this 14-electron complex to give the corresponding η^2-iminoacyl Zr complexes $[(C_5Me_4)SiMe_2(N\text{-}t\text{-}Bu)]ZrMe[\eta^2\text{-}C(Me)NR]$, **2**, and $[(C_5Me_4)SiMe_2(N\text{-}t\text{-}Bu)]Zr[\eta^2\text{-}C(Me)NR]_2$, **3**. Subsequent thermolysis of **3** leads to C,C-coupling of the two η^2-iminoacyl units and proceeds solely with formation of the enediamidate derivative $[(C_5Me_4)SiMe_2(N\text{-}t\text{-}Bu)]Zr[N(R)C(Me)=C(Me)N(R)]$, **4**. Compounds **2a**, **3a**−**c**, and **4a**−**c** have been observed and characterized by solution NMR measurements, and the molecular structures of **3a**, **3b**, **4a**, and **4b** have been confirmed by crystallographic methods. The nonplanar 1,4-diaza-5-zirconacyclopentene rings of **4a** and **4b** are folded by *ca.* 50° in opposite directions along the corresponding N···N line segment and adopt the prone and supine conformations, respectively. The activation parameters for the first-order intramolecular C,C-coupling reaction leading to the conversion of **3a** → **4a** are $\Delta H^{\ddagger} = 24.6(2)$ kcal/mol and $\Delta S^{\ddagger} = -11.3(7)$ eu and of **3b** → **4b** are $\Delta H^{\ddagger} = 23.9(3)$ kcal/mol and $\Delta S^{\ddagger} = -10.4(8)$ eu.

Introduction

Reactivity studies of the transition-metal-mediated reductive coupling of isocyanides by an electrophilic group 4 metal complex have uncovered two primary reaction mechanisms associated with this C−C bond forming reaction. From their studies of a series of bis(η^2-iminoacyl)aryloxide complexes, $M(OAr)_2[\eta^2\text{-}C(R')NR]_2$ (M = Ti, Zr, Hf), Rothwell and co-workers[1] observed that these compounds upon thermolysis undergo an intramolecular coupling of the two η^2-iminoacyl groups to produce the cyclic enediamidate complexes, $M(OAr)_2[N(R)C(R')=C(R')N(R)]$ (eq 1). Our investigations of the reductive coupling of isocyanides by "stabilized" group 4 metallacyclobutane complexes, $(C_5R_5)_2M(CH_2SiMe_2CH_2)$ (M = Zr,[2] Hf;[3] R = H, Me) revealed that this reaction proceeds via an unusual double insertion reaction that involves the participation of η^2-iminoacyl and η^2-iminoacyl imine intermediates (eq 2).

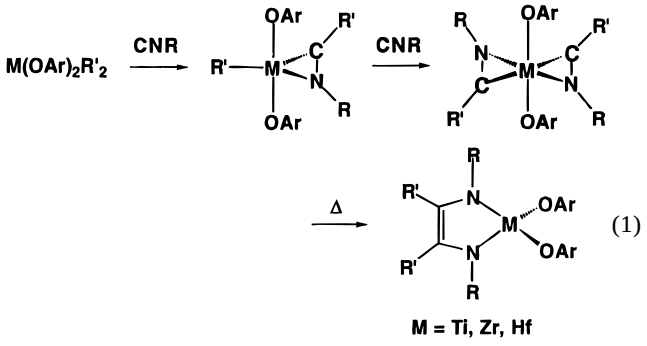

(1)

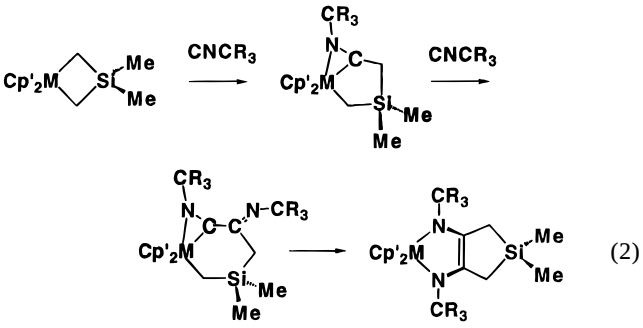

(2)

In the former case an isocyanide inserts sequentially into both M−C(alkyl) bonds, whereas in the latter case the electrophilic character of the η^2-iminoacyl carbon promotes nucleophilic attack of the second isocyanide

[⊗] Abstract published in *Advance ACS Abstracts,* July 1, 1997.

(1) (a) McMullen, A. K.; Rothwell, I. P.; Huffman, J. C. *J. Am. Chem. Soc.* **1985**, *107*, 1072. (b) Chamberlain, L. R.; Durfee, L. D.; Fanwick, P. E.; Kobriger, L. M.; Latesky, S. L.; McMullen, A. K.; Steffey, B. D.; Rothwell, I. P.; Folting, K.; Huffman, J. C. *J. Am. Chem. Soc.* **1987**, *109*, 6068. (c) Durfee, L. D.; Rothwell, I. P. *Chem. Rev.* **1988**, *88*, 1059 and references cited therein.

(2) (a) Berg, F. J.; Petersen, J. L. *Organometallics* **1989**, *8*, 2461. (b) Berg, F. J.; Petersen, J. L. *Organometallics* **1991**, *10*, 1599. (c) Berg, F. J.; Petersen, J. L. *Tetrahedron* **1992**, *48*, 4749. (d) Valero, C.; Grehl, M.; Wingbermühle, D.; Kloppenburg, L.; Carpenetti, D.; Erker, G.; Petersen, J. L. *Organometallics* **1994**, *13*, 415.

(3) (a) Berg, F. J.; Petersen, J. L. *Organometallics* **1993**, *12*, 3890. (b) Kloppenburg, L.; Petersen, J. L. *Polyhedron* **1995**, *14*, 69.

S0276-7333(96)01076-X CCC: $14.00

at this carbenium-type[4] carbon center. Isocyanide insertion into the remaining metal−carbon bond of the η^2-iminoacyl intermediate is not observed. Similarly, isocyanide insertion into only one metal−carbon bond occurs for the related d^0 Zr(IV) complexes $(C_5R_5)_2$-$Zr(alkyl)_2$, R = H, Me.[5]

The observed differences in these two C,C-coupling pathways are primarily a consequence of the level of coordinative unsaturation at the early transition metal center in the 12-electron bis(aryloxide) complexes, $M(OAr)_2R'_2$, and in the 16-electron $(C_5R_5)_2Zr(alkyl)_2$ and $(C_5R_5)_2M(CH_2SiMe_2CH_2)$ complexes. The presence of only one vacant metal orbital in these 16-electron complexes led us to hypothesize that a prerequisite for the direct coupling of two iminoacyl fragments is the availability of a minimum of two vacant orbitals at the electrophilic d^0 group 4 metal center.[6]

Several years ago, Bercaw and co-workers[7] demonstrated that the incorporation of the bifunctional *ansa*-monocyclopentadienylamido ligand $[(C_5Me_4)SiMe_2(N\text{-}t\text{-}Bu)]^{2-}$ provides an effective strategy for enhancing the Lewis acidity of d^0 organoscandium complexes. Replacement of a permethylated cyclopentadienyl ring with an appended amido functionality simultaneously reduces steric crowding and lowers the metal's formal electron count by two, thus generating another vacant metal orbital. Researchers at Dow Chemical Co. and Exxon later independently found that the corresponding d^0 group 4 metal complexes $[(\eta^5\text{-}C_5R_4)SiR'_2(\eta^1\text{-}NR'')]ML_2$ (M = Ti, Zr, Hf; R = H, alkyl; R′,R″ = alkyl, aryl; L = Cl, Me) in the presence of excess methylalumoxane provide commercially viable Ziegler−Natta catalysts for the copolymerization of ethylene and 1-alkenes.[8]

Although the spotlight on 14-electron *ansa*-monocyclopentadienylamido group 4 metal complexes, such as $[(C_5Me_4)SiMe_2(N\text{-}t\text{-}Bu)]ZrMe_2$, remains primarily focused on their industrial application, far less in known about their reactivity with unsaturated substrates.[9] To provide an operational test of our working hypothesis, we have undertaken an investigation of the migratory insertion reaction of $[(C_5Me_4)SiMe_2(N\text{-}t\text{-}Bu)]ZrMe_2$, **1**, with various isocyanides. We have found that these reactions indeed proceed with the formation of the corresponding bis(η^2-iminoacyl) complexes $[(C_5Me_4)SiMe_2(N\text{-}t\text{-}Bu)]Zr[\eta^2\text{-}C(Me)NR]_2$, **3**, which upon thermolysis rearrange to the enediamido isomer $[(C_5Me_4)SiMe_2(N\text{-}t\text{-}Bu)]Zr[N(R)C(Me)=C(Me)N(R)]$, **4**. Specific details regarding the relevant kinetic and structural aspects of the migratory insertion and intramolecular isocyanide coupling reactions displayed by $[(C_5Me_4)SiMe_2(N\text{-}t\text{-}Bu)]ZrMe_2$ are described herein.

Experimental Section

Reagents. Reagent grade hydrocarbon and ethereal solvents were purified using standard methods and distilled under nitrogen. Na/K alloy was used to dry pentane, toluene, and tetrahydrofuran. These dried solvents were then transferred to storage flasks containing $[(C_5H_5)_2Ti(\mu\text{-}Cl)_2]_2Zn$[10] and were freshly distilled prior to use. Hexamethyldisiloxane and diethyl ether were dried over CaH_2. Chlorinated solvents were distilled from P_4O_{10}. The deuterated solvents, C_6H_6-d_6 (Aldrich, 99.5%) and $CDCl_3$ (Aldrich, 99.8%), were dried over activated 4 Å molecular sieves prior to use; *tert*-butyl isocyanide (Aldrich), t-butylamine (Aldrich), and $SiMe_2Cl_2$ (Hüls) were also stored over 4 Å molecular sieves and then introduced by vacuum transfer. Methyllithium (Aldrich, 1.4 M in diethyl ether) and 2,6-xylyl isocyanide (Fluka) were used as received, whereas CNMe[11] and $[(C_5Me_4)SiMe_2(N\text{-}t\text{-}Bu)]ZrCl_2$[12] were prepared employing literature procedures.

General Considerations. All manipulations and reactions were carried out on a double-manifold, high-vacuum line or in a Vacuum Atmospheres glovebox equipped with a HE-493 Dri-Train. Air- and moisture-sensitive compounds were synthesized using pressure equalizing filter frits equipped with high-vacuum Teflon stopcocks. Nitrogen was purified by passage over reduced BTS catalysts and activated 4 Å molecular sieves. All glassware was thoroughly oven-dried or flame-dried under vacuum prior to use. NMR sample tubes were sealed under approximately 500 Torr of nitrogen. The NMR spectra were acquired using procedures and instrumentation that has been previously described.[2b] The NMR assignments for the different methyl protons in **1**, **3a**, **3b**, **4a**, and **4b** were made on the basis of the cross peaks observed in the corresponding HETCOR NMR spectrum. Elemental analyses were performed either by Robertson Microlit Laboratories, Madison, NJ (RML), or by E+R Microanalytical Laboratory, Corona, NY (E+R).

Synthesis of $[(C_5Me_4)SiMe_2(N\text{-}t\text{-}Bu)]ZrMe_2$, 1. A solution of $[(C_5Me_4)SiMe_2(N\text{-}t\text{-}Bu)]ZrCl_2$ (0.75 g, 1.82 mmol) in diethyl ether (50 mL) was cooled down to −78 °C. Methyllithium (3.0 mL, 4.20 mmol) was added dropwise via syringe under a N_2 flush. A white precipitate formed, and the reaction mixture was stirred overnight at room temperature. The solvent was replaced by an equal volume of pentane, and the soluble product was separated from LiCl by filtration. After removal of the pentane, sublimation (10^{-4} Torr, 60 °C) of the crude product yielded a white semicrystalline material. Yield: 0.45 g (76%). ^{1}H NMR (C_6H_6-d_6): δ 1.97, 1.91 (C_5Me_4, s), 1.40 ($NCMe_3$, s), 0.46 ($SiMe_2$, s), −0.01 ($ZrMe_2$, s); ($CDCl_3$) δ 2.08, 1.98 (C_5Me_4, s), 1.42 ($NCMe_3$, s), 0.44 ($SiMe_2$, s), −0.39 ($ZrMe_2$, s). ^{13}C NMR (C_6H_6-d_6, mult., $^1J_{CH}$ in Hz): δ 130.2, 125.3 (proximal and distal carbons of C_5Me_4, s), 95.8 (bridgehead carbon of C_5Me_4, s), 54.9 ($NCMe_3$, s), 35.8 (ZrMe, q, 114), 34.4 ($NCMe_3$, q, 125), 14.3, 11.3 (C_5Me_4, q, 127), 6.65 ($SiMe_2$, q, 118). The ^{1}H and ^{13}C NMR chemical shifts are comparable to those reported in ref 8d. Anal. Calcd for $C_{17}H_{33}NSiZr$ (370.76): C, 55.07; H, 8.97; N, 3.78. Found: C, 55.19; H, 9.15; N, 3.78 (E+R).

(4) Tatsumi, K.; Nakamura, A.; Hofmann, P.; Stauffert, P.; Hoffmann, R. *J. Am. Chem. Soc.* **1985**, *107*, 4440.

(5) (a) Lappert, M. F.; Luong-Thi, N. T.; Milne, C. R. C. *J. Organomet. Chem.* **1979**, *174*, C35. (b) Wolczanski, P. T.; Bercaw, J. E. *J. Am. Chem. Soc.* **1979**, *101*, 6450. (c) Lyszak, E. L.; O'Brien, J. P.; Kort, D. A.; Hendges, S. K.; Redding, R. N.; Bush, T. L.; Hermen, M. S.; Renkema, K. B.; Silver, M. E.; Huffman, J. C. *Organometallics* **1993**, *12*, 338.

(6) Notable examples of the C,C-coupling of isocyanides by an electrophilic group 4 metal complex not involving the direct coupling of two η^2-iminoacyls include: (a) Bocarsly, J. R.; Floriani, C.; Chiesa-Villa, A.; Guastini, C. *Organometallics* **1986**, *5*, 2380. (b) Hessen, B.; Blenkers, J.; Teuben, J. H.; Helgesson, G.; Jagner, S. *Organometallics* **1989**, *8*, 830. (c) Fandos, R.; Meetsma, A.; Teuben, J. H. *Organometallics* **1991**, *10*, 2665.

(7) (a) Shapiro, P. J.; Bunel, E. E.; Schaefer, W. P.; Bercaw, J. E. *Organometallics* **1990**, *9*, 867. (b) Piers, W. E.; Shapiro, P. J.; Bunel, E. E.; Bercaw, J. E. *Synlett* **1990**, *2*, 74. (c) Shapiro, P. J.; Cotter, W. D.; Schaefer, W. P.; Labinger, J. A.; Bercaw, J. E. *J. Am. Chem. Soc.* **1994**, *116*, 4623.

(8) (a) Canich, J. M. Eur. Pat. Appl. EP-420-436-A1, 1990. (b) Canich, J. M. U.S. Patent 5,026,798, 1991. (c) Canich, J. M.; Hlatky, G. G.; Turner, H. W. PCT Int. Appl. WO92-00333, 1992. (d) Stevens, J. C.; Timmers, F. J.; Wilson, D. R.; Schmidt, G. F.; Nickias, P. N.; Rosen, R. K.; Knight, G. W.; Lai, S. Eur. Pat. Appl. EP-416-815-A2, 1991. (e) Campbell, R. E., Jr. U.S. Patent 5,066,741, 1991. (f) LaPointe, R. E. European Patent 468651, 1991.

(9) Kloppenburg, L; Petersen, J. L. *Organometallics* **1996**, *15*, 7.

(10) Setukowski, D. G.; Stucky, G. D. *Inorg. Chem.* **1975**, *14*, 2192.

(11) Schuster, R. E.; Scott, J. E.; Casanova, J., Jr. *Org. Synth.* **1973**, *5*, 773.

(12) Carpenetti, D. W.; Kloppenburg, L.; Kupec, J. T.; Petersen, J. L. *Organometallics* **1996**, *15*, 1572.

Synthesis of [(C_5Me_4)$SiMe_2$(N-t-Bu)]Zr[η^2-C(Me)N(t-Bu)]$_2$, 3a. Initially, this reaction was performed in a sealed NMR tube. Two equiv of *tert*-butyl isocyanide were added to a solution of **1** (0.032 g, 0.086 mmol) in benzene-d_6. Periodic NMR measurements indicated that the reaction proceeds initially with rapid insertion of 1 equiv of CN-t-Bu to give the η^2-iminoacyl adduct [(C_5Me_4)$SiMe_2$(N-t-Bu)]ZrMe[η^2-C(Me)N(t-Bu)], **2a**, and eventually the diinsertion product, **3a**, by taking up the second equivalent of CN-t-Bu after 1 day. Because this double isocyanide insertion reaction yields a single product, it was repeated on a larger scale. A 25 mL pentane solution of **1** (0.90 g, 2.43 mmol) was charged with nearly 3 equiv of CN-t-Bu (0.80 mL, 7.08 mmol). The yellow reaction mixture was stirred at ambient temperature for 6 days. Following solvent removal, the product was washed with hexamethyldisiloxane (2 × 5 mL). Slow removal of pentane from a pentane solution of **3a** yielded pale yellow crystals suitable for an X-ray diffraction analysis. Isolated yield: 1.194 g (91%).

Monoinsertion product, **2a**: ^{1}H NMR (C_6H_6-d_6) δ 2.45, 2.26, 1.89 (proximal and distal protons of C_5Me_4 and η^2-CMe, s), 1.19, 1.09 ($NCMe_3$, s), 0.69, 0.70 ($SiMe_2$, s), 0.04 (ZrMe, s). ^{13}C NMR (C_6H_6-d_6, mult., $^1J_{CH}$ in Hz): δ 247.9 (η^2-C, s), 122.3, 121.8 (proximal and distal carbons of C_5Me_4, s), 100.2 (bridgehead carbon of C_5Me_4, s), 62.4 (Zr$NCMe_3$, s), 54.5 (Si$NCMe_3$, s), 34.3 (SiNCMe_3, q, 126), 30.3 (ZrNCMe_3, q, 126), 23.0 (η^2-C*Me*, q, 127), 20.2 (ZrMe, q, 113), 14.8, 11.3 (C_5Me_4, q, 126), 7.43, 7.28 ($SiMe_2$, q, 118).

Diinsertion product, **3a**: ^{1}H NMR (C_6H_6-d_6) δ 2.36, 1.76 (proximal and distal protons of C_5Me_4), 2.35 (η^2-CMe, s), 1.34 ($SiNCMe_3$, s), 1.22 ($ZrNCMe_3$, s), 0.79 ($SiMe_2$, s). ^{13}C NMR (C_6H_6-d_6, mult., $^1J_{CH}$ in Hz): δ 246.0 (η^2-C, s), 123.8, 122.4 (proximal and distal carbons of C_5Me_4, s), 104.0 (bridgehead carbon of C_5Me_4, s), 58.9 (Zr$NCMe_3$, s), 53.8 (Si$NCMe_3$, s), 36.1 (SiNCMe_3, q, 126), 30.7 (ZrNCMe_3, q, 126), 23.4 (η^2-C*Me*, q, 126), 15.2, 12.0 (C_5Me_4, q, 126), 8.94 ($SiMe_2$, q, 118). Anal. Calcd for $C_{27}H_{51}N_3SiZr$ (537.03): C, 60.39; H, 9.57; N, 7.82. Found: C, 60.39; H, 9.59; N, 7.67 (E+R).

Synthesis of [(C_5Me_4)$SiMe_2$(N-t-Bu)]Zr[N(t-Bu)C(Me)=C(Me)N(t-Bu)], 4a. A sample of **3a** (0.035 g, 0.065 mmol) was added to a NMR tube and dissolved in benzene-d_6. Periodic ^{1}H NMR measurements indicated that **3a** upon heating rearranges solely to **4a**. On a larger scale, a cylindrical reaction tube equipped with a high-vacuum adapter was charged with **3a** (0.232 g, 0.43 mmol) and 10 mL of toluene. The solution was heated to 70 °C for 9 days. The solvent was removed, and the product was extracted with pentane to give a yellow crystalline material. Slow removal of pentane from a saturated pentane solution of **4a** afforded single crystals suitable for X-ray structural analysis. Yield: 0.227 g (98%). ^{1}H NMR (C_6H_6-d_6): δ 2.37, 1.53 (proximal and distal methyl protons of C_5Me_4, s), 1.95 (=CMe, s), 1.37 ($ZrNCMe_3$, s), 1.34 ($SiNCMe_3$, s), 0.80 ($SiMe_2$, s). ^{13}C NMR (C_6H_6-d_6, mult., $^1J_{CH}$ in Hz): δ 125.0, 122.5 (proximal and distal carbons of C_5Me_4, s), 109.0 (=C, s), 104.2 (bridgehead carbon of C_5Me_4, s), 55.9 (Zr$NCMe_3$, s), 55.7 (Si$NCMe_3$, s), 35.3 (SiNCMe_3, q, 124), 34.2 (ZrNCMe_3, q, 125), 19.9 (=C*Me*, q, 126), 15.4, 11.5 (C_5Me_4, q, 126), 8.81 ($SiMe_2$, q, 118). Anal. Calcd for $C_{27}H_{51}N_3SiZr$ (537.03): C, 60.39; H, 9.57; N, 7.82. Found: C, 60.18; H, 9.66; N, 7.63 (RML).

Synthesis of [(C_5Me_4)$SiMe_2$(N-t-Bu)]Zr[η^2-C(Me)N(2,6-xylyl)]$_2$, 3b. A NMR tube was charged with **1** (0.030 g, 0.081 mmol) and 2,6-xylyl isocyanide (0.027 g, 0.206 mmol). The solids were dissolved in deuterated chloroform. ^{1}H NMR measurements indicate that the isocyanide insertion reaction proceeds at ambient temperature with formation of **3b**. On a larger scale, a 25 mL pentane solution of **1** (0.72 g, 1.94 mmol) and 2,6-xylyl isocyanide (0.60 g, 4.57 mmol) was stirred at ambient temperature for 9 days. The solvent was filtered, and the product was washed with pentane (2 × 25 mL), yielding **3b** as a white powder. Slow removal of solvent from a toluene solution yielded single crystals suitable for X-ray analysis. Yield: 0.984 g (80%). ^{1}H NMR ($CDCl_3$): δ 6.96−6.90 (*meta* and *para* CH, m), 2.30, 1.97 (proximal and distal methyl protons of C_5Me_4, s), 1.93, 1.63 (methyl protons of 2,6-xylyl groups, s), 2.18 (η^2-CMe, s), 0.96 ($NCMe_3$, s), 0.51 ($SiMe_2$, s). ^{1}H NMR (C_6H_6-d_6): δ 6.91−6.85 (*meta* and *para* CH, m), 2.37, 1.85 (proximal and distal methyl protons of C_5Me_4, s), 1.96, 1.66 (methyl protons of 2,6-xylyl groups, s), 2.02 (η^2-CMe, s), 1.21 ($NCMe_3$, s), 0.79 ($SiMe_2$, s). ^{13}C NMR ($CDCl_3$, mult., $^1J_{CH}$ in Hz): δ 251.8 (η^2-*C*, s), 147.2 (N*C*, s), 129.2, 128.6 (xylyl-*C*Me, s), 127.9, 127.7, 124.3 (*meta* and *para* CH, d, 156, 156, 160), 123.5, 122.8 (proximal and distal carbons of C_5Me_4, s), 104.8 (bridgehead carbon of C_5Me_4, s), 55.0 ($NCMe_3$, s), 35.5 (NCMe_3, q, 124), 23.8 (η^2-C*Me*, q, 126), 19.7, 17.6 (xylyl-C*Me*, q, 127), 14.6, 11.6 (C_5Me_4, q, 126), 8.09 ($SiMe_2$, q, 118). Anal. Calcd for $C_{35}H_{51}N_3SiZr$ (633.12): C, 66.40; H, 8.12; N, 6.64. Found: C, 66.48; H, 8.22; N, 6.60 (E+R).

Synthesis of [(C_5Me_4)$SiMe_2$(N-t-Bu)]Zr[N(2,6-xylyl)C(Me)=C(Me)N(2,6-xylyl)], 4b. A NMR tube containing the solution of **3b** in deuterated chloroform was heated in an oil bath at 75 °C. Periodic ^{1}H NMR measurements revealed that **3b** rearranges solely to **4b**. On a larger scale, a cylindrical reaction tube equipped with a high-vacuum adapter was charged with **3b** (0.235 g, 0.371 mmol) and toluene (10 mL). The solution was stirred at 70 °C for 2 days. After the solvent was removed, the product residue was washed with pentane (5 mL). Yellow single crystals of **4b** suitable for X-ray diffraction studies were obtained by slow removal of the solvent from a saturated toluene solution. Yield: 0.167 g (71%). ^{1}H NMR ($CDCl_3$): δ 7.12−6.92 (*meta* and *para* CH, m), 2.37 (=CMe, s), 1.97, 1.36 (C_5Me_4, s), 1.88, 1.68 (xylyl-CMe, s), 1.07 ($NCMe_3$, s), 0.62 ($SiMe_2$, s). ^{13}C NMR ($CDCl_3$, mult., $^1J_{CH}$ in Hz): δ 148.3 (xylyl-N*C*, s), 134.5, 132.9 (xylyl-*C*Me, s), 128.6, 128.2 (proximal and distal carbons of C_5Me_4, s), 128.0, 127.6, 123.6 (*meta* and *para* CH, d, 156, 154, 160), 112.8 (=C, s), 100.1 (bridgehead carbon of C_5Me_4, s), 55.6 ($NCMe_3$, s), 34.4 (NCMe_3, q, 125), 21.8 (=C*Me*, q, 126), 19.4, 17.0 (xylyl-C*Me*, q, 127), 13.6, 9.56 (C_5Me_4, q, 127), 8.34 ($SiMe_2$, q, 118). Anal. Calcd for $C_{35}H_{51}N_3SiZr$ (633.12): C, 66.40; H, 8.12; N, 6.64. Found: C, 66.34; H, 8.22; N, 6.59 (E+R).

Reductive Coupling of CNMe. A NMR sample tube equipped with a calibrated gas bulb was charged with **1** (0.030 g, 0.081 mmol) and benzene-d_6. Two equivalents of methyl isocyanide were then introduced. The reaction mixture turned dark brown after a few hours. NMR measurements confirmed the formation of the bis(η^2-iminoacyl) product **3c**, which gives a characteristic downfield ^{13}C NMR resonance at δ 242.2. ^{1}H NMR (C_6H_6-d_6): δ 2.79 (NMe, s), 2.28, 1.97, 1.79 (proximal and distal methyl protons of C_5Me_4 and η^2-CMe, s), 1.37 ($NCMe_3$, s), 0.77 ($SiMe_2$, s). ^{13}C{^{1}H} NMR (C_6H_6-d_6): δ 242.2 (η^2-C), 124.0, 123.3 (proximal and distal carbons of C_5Me_4), 90.1 (bridgehead carbon of C_5Me_4), 54.1 (N*C*Me_3), 35.8 (NC-*Me*$_3$), 35.6 (NMe), 19.6 (η^2-C*Me*), 14.4, 11.6 (C_5Me_4), 8.96 ($SiMe_2$). Upon heating the NMR sample tube containing **3c** to 65 °C, the proton NMR resonances of the η^2-iminoacyl product **3c** diminished with the formation of the enediamido isomer, **4c**. ^{1}H NMR (C_6H_6-d_6): δ 3.16 (NMe, s), 2.29, 1.88, 1.71 (proximal and distal protons of C_5Me_4 and =CMe, s), 1.09 ($NCMe_3$, s), 0.73 ($SiMe_2$, s).

Kinetic Measurements. The first-order thermal rearrangements of **3a** → **4a** and of **3b** → **4b** were followed by monitoring the loss of the intensity of the ^{1}H NMR resonance corresponding to the t-Bu substituents of the η^2-iminoacyl ligands located at δ 1.22 for **3a** and the t-Bu substituent of the appended amido at δ 1.21 for **3b**. Two standard solutions were prepared by dissolving 0.537g of **3a** and 0.186 g of ferrocene in 8.773 g of C_6D_6 (0.108 M) and by adding 0.3168 g of **3b** and 0.0931 g of ferrocene to 8.332 g of C_6D_6 (0.0571 M). Appropriate aliquots taken from each solution were sealed in a series of NMR tubes. A typical kinetic run involved submerging the NMR tube in an oil bath set at an appropriate temperature (within the range 70−120 °C) maintained to ±0.1

Table 1. Rate Constants for the Intramolecular Rearrangement of 3a → 4a and 3b → 4b

T, °C	*k*, s^{-1}	$t_{1/2}$, min
	3a → 4a	
70.0	$5.21(4) \times 10^{-6}$	2215(17)
80.0	$1.54(1) \times 10^{-5}$	750(5)
90.0	$4.40(4) \times 10^{-5}$	262(2)
100.0	$1.09(2) \times 10^{-4}$	106(2)
110.0	$2.53(2) \times 10^{-4}$	45.7(4)
120.0	$5.95(11) \times 10^{-4}$	19.4(4)
	3b → 4b	
70.0	$2.26(6) \times 10^{-5}$	511(14)
80.0	$6.60(8) \times 10^{-5}$	175(2)
90.0	$1.67(2) \times 10^{-4}$	69.4(8)
100.0	$4.26(8) \times 10^{-4}$	27.1(5)
110.0	$1.06(2) \times 10^{-3}$	10.9(2)
120.0	$2.16(6) \times 10^{-3}$	5.3(2)

°C with a Fisher Scientific model 730 isotemp immersion circulator. The NMR tube was removed from the oil bath at a predetermined time and then immediately cooled in an ice-water slush bath to quench the rearrangement reaction. Each ^{1}H NMR spectrum was measured three times with a pulse delay of 20 s in order to obtain reliable peak integrations. The integrated intensity for the *tert*-butyl proton resonance obtained for these three spectra was reproducible to within 5%; the averaged integrated peak intensity for each run was used in the determination of the rate constant *k* at each temperature. The sample was then returned to the constant-temperature oil bath, and the process was repeated for a total time corresponding to a minimum of at least three half-lives. The concentrations of **3a** and **3b** were calculated from the expressions:

$$[\mathbf{3a}] = \frac{10(\text{area of iminoacyl t-Bu resonance of } \mathbf{3a})}{18(\text{area of Cp resonance of } Cp_2Fe)}[Cp_2Fe]$$

and

$$[\mathbf{3b}] = \frac{10(\text{area of appended amido t-Bu resonance of } \mathbf{3b})}{9(\text{area of Cp resonance of } Cp_2Fe)}[Cp_2Fe]$$

The experimentally determined rate constants and $t_{1/2}$ values for the rearrangements **3a** → **4a** and **3b** → **4b** are summarized in Table 1. The values of the activation parameters, $\Delta H^{\ddagger}$ and $\Delta S^{\ddagger}$, were calculated from the least-squares determined slope ($\Delta H^{\ddagger}/R$) and the *y*-intercept ($-\Delta S^{\ddagger}/R - 23.76$), respectively, of the corresponding plot of $-\ln(k/T)$ vs $1/T$, assuming a transmission coefficient of unity in the Eyring equation $\Delta G^{\ddagger}(T) = RT\ln(\kappa k_B T/kh)$, Figure 1. The standard errors, which are given in parentheses for the activation parameters, correspond to the errors calculated from the regression analysis.[13]

X-ray Data Collection and Structural Analyses of 3a, 3b, 4a, and 4b. The molecular structures of **3a**, **3b**, **4a**, and **4b** were determined following the same general procedure for each X-ray structural analysis. A suitable crystal was sealed in a capillary tube under a nitrogen atmosphere and then optically aligned on the goniostat of a Siemens P4 automated X-ray diffractometer. The unit cell dimensions were initially determined by indexing a set of reflections whose angular coordinates were obtained either from a rotation photograph or with the automatic peak search routine provided with XSCANS.[14] The corresponding unit cell parameters and orientation matrix were determined from a nonlinear least-squares fit of the orientation angles of at least 20 higher order reflections at 22 °C. The refined lattice parameters and other pertinent crystallographic information are summarized in Table 2.

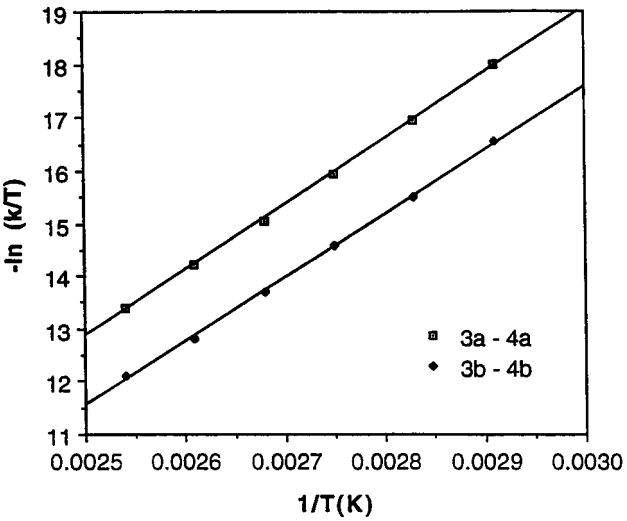

Figure 1. Eyring plots for the first-order intramolecular rearrangements of **3a** to **4a** and **3b** to **4b**.

Intensity data were measured with graphite-monochromated Mo Kα radiation ($\lambda = 0.710\ 73$ Å) and variable ω scans. Background counts were measured at the beginning and at the end of each scan with the crystal and counter kept stationary. The intensities of three standard reflections were measured after every 100 reflections. The intensity data were corrected for Lorentz−polarization and crystal decay (when appropriate). An empirical absorption correction (when applied) was based upon ψ scans measured for a minimum of eight reflections with $\chi \approx \pm 90°$ and 2θ ranging from 5° to 45°.

The structure solution in each case was provided by the first *E*-map calculated on the basis of the phase assignments made by the SHELXTL direct methods structure solution software. The coordinates of all remaining non-hydrogen atoms that were not revealed on the initial *E*-map were located in the subsequent difference Fourier map. All hydrogen atoms were idealized with isotropic temperature factors set at 1.2 times that of the adjacent carbon. The positions of all the methyl hydrogens were optimized by a rigid rotating group refinement with idealized tetrahedral angles. Full-matrix least-squares refinement, based upon the minimization of $\sum w_i|F_o^2 - F_c^2|^2$, with $w_i^{-1} = [\sigma^2(F_o^2) + (aP)^2 + bP]$ where $P = (\text{Max}(F_o^2,0) + 2F_c^2)/3$, was performed with SHELXL-93[15] operating on a Silicon Graphics Iris Indigo workstation. The final values of the discrepancy indices are provided in Table 2. Their values were calculated from the expressions $R1 = \sum||F_o| - |F_c||/\sum|F_o|$ and $wR2 = [\sum(w_i(F_o^2 - F_c^2)^2)/\sum(w_i(F_o^2)^2)]^{1/2}$, and the standard deviation of an observation of unit weight σ_1 is equal to $[\sum(w_i(F_o^2 - F_c^2)^2)/(n - p)]^{1/2}$, where *n* is the number of reflections and *p* is the number of parameters varied during the last refinement cycle.

Selected interatomic distances and bond angles for the bis(η^2-iminoacyl) compounds, **3a** and **3b**, and for the cyclic enediamidate complexes, **4a** and **4b**, are compared in Tables 3 and 4, respectively.

Discussion of Results

Migratory Isocyanide Insertion and C,C-Coupling Reactions. The reactions of 2 equiv of CNR (R

(13) Skoog, D. A.; West , D. M.; Holler, F. J. *Analytical Chemistry, an Introduction*, 6th ed.; Saunders College Publishing: Philadelphia, PA, 1994; Appendix 6.

(14) XSCANS (version 2.0) is a diffractometer control system developed by Siemens Analytical X-ray Instruments, Madison, WI.

(15) SHELXL-93 is a FORTRAN-77 program developed by Professor G. Sheldrick (Institut für Anorganische Chemie, University of Göttingen, D-37077 Göttingen, Germany) for single-crystal X-ray structural analyses.

Table 2. Crystallographic Data for the X-ray Structural Analyses of [(C_5Me_4)$SiMe_2$(N-t-Bu)]Zr[η^2-C(Me)NR]$_2$ (R = *tert*-Butyl (3a), 2,6-Xylyl (3b), and [(C_5Me_4)$SiMe_2$(N-t-Bu)]Zr[NRC(Me)=C(Me)NR] (R = *tert*-Butyl (4a), 2,6-Xylyl (4b))

	A. Crystal Data			
compound	**3a**	**3b**	**4a**	**4b**
emp form	$C_{27}H_{51}N_3SiZr$	$C_{35}H_{51}N_3SiZr$	$C_{27}H_{51}N_3SiZr$	$C_{35}H_{51}N_3SiZr$
dimens, mm	0.20 × 0.40 × 0.60	0.36 × 0.40 × 0.48	0.20 × 0.30 × 0.54	0.20 × 0.30 × 0.42
cryst syst	orthorhombic	triclinic	orthorhombic	monoclinic
space group	*Pbca*	$P\bar{1}$	*Pbca*	$P2_1/c$
a, Å	16.957(1)	11.4096(8)	11.968(1)	16.282(1)
b, Å	11.979(1)	12.0530(9)	17.738(1)	10.611(1)
c, Å	30.469(3)	13.2952(10)	27.679(2)	19.544(1)
α, deg	90	83.642(6)	90	90
β, deg	90	79.413(6)	90	93.352(7)
γ, deg	90	72.010(6)	90	90
volume, Å^3	6189.1(7)	1706.5(2)	5875.9(8)	3370.8(4)
Z	8	2	8	4
fw	537.03	633.12	537.03	633.12
density, g/cm^3	1.153	1.232	1.214	1.248
μ, cm^{-1}	4.11	3.84	4.33	3.88
F(000)	2304	672	2304	1344
	B. Data Collection and Structural Analyses			
scan type	*ω*, variable	*ω*, variable	*ω*, variable	*ω*, variable
scan rate, deg/min	2.0−10.0	2.0−10.0	3.0−10.0	2.0−10.0
2*θ* range, deg	3.0−50.0	3.0−50.0	3.0−50.0	3.0−50.0
reflns sampled	h ($-1 \le h \le 20$)	h ($-13 \le h \le 12$)	h ($-1 \le h \le 14$)	h ($0 \le h \le 19$)
	k ($-1 \le k \le 14$)	k ($-14 \le k \le 0$)	k ($-1 \le k \le 21$)	k ($0 \le k \le 12$)
	l ($-36 \le l \le 1$)	l ($-15 \le l \le 15$)	l ($-1 \le l \le 32$)	l ($-23 \le l \le 23$)
no. of reflns	6636	6308	6294	6097
no. of unique data	5433	5990	5137	5879
agreement factor	R_{int} = 0.0375	R_{int} = 0.0180	R_{int} = 0.0429	R_{int} = 0.0226
no. of data ($I > 2\sigma(I)$)	4601	5711	4330	5295
abs corr	empirical	empirical	none	empirical
R indices ($I > 2\sigma(I)$)	R1 = 0.0497	R1 = 0.0328	R1 = 0.0517	R1 = 0.0420
	wR2 = 0.0904	wR2 = 0.0750	wR2 = 0.0860	wR2 = 0.0812
R indices for all data	R1 = 0.1182	R1 = 0.0453	R1 = 0.1257	R1 = 0.0808
	wR2 = 0.1155	wR2 = 0.0809	wR2 = 0.1097	wR2 = 0.0964
σ_1, GOF	1.032	1.026	1.006	1.001
values of *a* and *b*	0.0437, 0.0	0.0384, 0.67	0.0338, 0.0	0.0411, 0.0
no. of variables	307	376	307	376
data to parameter ratio	17.7:1	15.2:1	16.7:1	14.1:1
largest diff peak and hole	0.254, −0.284	0.232, −0.209	0.336, −0.279	0.241, −0.217

= (**a**) *tert*-butyl, (**b**) 2,6-xylyl, (**c**) Me) with [(C_5Me_4)-$SiMe_2$(N-t-Bu)]$ZrMe_2$, **1**, similarly proceed at 25 °C with the sequential migratory insertion of an equivalent of isocyanide into each Zr−C(Me) bond (eq 3) to afford the mono(η^2-iminoacyl) and bis(η^2-iminoacyl) complexes [(C_5Me_4)$SiMe_2$(N-t-Bu)]ZrMe[η^2-C(Me)NR], **2**, and [(C_5-Me_4)$SiMe_2$(N-t-Bu)]Zr[η^2-C(Me)NR]$_2$, **3**. For *tert*-butyl

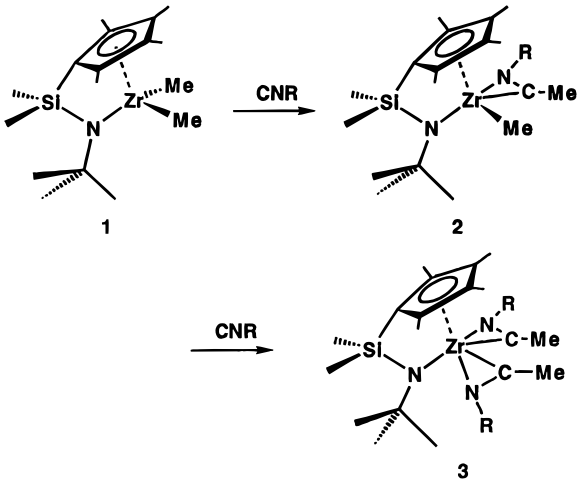

(3)

isocyanide, this insertion reaction proceeds sufficiently slow to observe the formation of the intermediate mono (η^2-iminoacyl) complex, **2a**, which was identified in solution by the presence of a characteristic downfield ^{13}C NMR resonance for the η^2-iminoacyl carbon nucleus at δ 247.9. Whereas two resolved ^1H and ^{13}C NMR resonances for the diastereotopic methyl groups of the $SiMe_2$ linkage are observed for **2a**, only two rather than the expected four ^1H and ^{13}C NMR resonances are observed for the proximal and distal methyl groups and the ring carbon atoms. This latter observation may reflect the presence of a dynamic process involving the methyl and η^2-iminoacyl ligands of **2a**. The bis(η^2-iminoacyl) species **3a**−**c** also exhibit a single downfield ^{13}C NMR resonance in solution for the two η^2-iminoacyl carbons, consistent either with a C_s-symmetric static structure in which both iminoacyls adopt the sterically more favorable N-outside orientation or with a dynamic structure that has the N-inside and N-outside conformations rapidly interconverting on the NMR time scale. The results of the X-ray structure determinations performed on **3a** and **3b** (vide infra) indicate that the two η^2-iminoacyl ligands do not adopt the C_s-symmetric structure in the solid state.

Upon thermolysis, the bis(η^2-iminoacyl) complexes **3a**−**c** rearrange via an intramolecular reaction that involves C,C-coupling of the two iminoacyl ligands to afford solely the cyclic enediamido complexes, **4a**−**c**, respectively (eq 4). These reactions proceed with concomitant disappearance of the downfield η^2-iminoacyl carbon resonance of **3a**−**c**. The activation parameters for the first-order conversions of **3a** → **4a** and **3b** → **4b**

Table 3. Selected Interatomic Distances (Å) and Bond Angles (deg) for the Bis(η^2-iminoacyl)zirconium Complexes 3a and 3b[a,b]

3a		3b	
A. Interatomic Distances			
Zr−Cp(c)	2.231	Zr−Cp(c)	2.236
Zr−N(1)	2.184(3)	Zr−N(1)	2.174(2)
Zr−N(2)	2.235(4)	Zr−N(2)	2.316(2)
Zr−N(3)	2.304(4)	Zr−N(3)	2.268(2)
Zr−C(16)	2.218(5)	Zr−C(16)	2.258(3)
Zr−C(22)	2.242(5)	Zr−C(26)	2.237(3)
Si−C(1)	1.863(5)	Si−C(1)	1.871(3)
Si−N(1)	1.711(4)	Si−N(1)	1.716(2)
N(1)−C(12)	1.485(5)	N(1)−C(12)	1.485(3)
N(2)−C(16)	1.276(6)	N(2)−C(16)	1.282(3)
N(3)−C(22)	1.259(6)	N(3)−C(26)	1.276(3)
N(2)−C(18)	1.504(6)	N(2)−C(18)	1.434(3)
N(3)−C(24)	1.508(6)	N(3)−C(28)	1.434(3)
B. Bond Angles			
Cp(c)−Zr−N(1)	99.2	Cp(c)−Zr−N(1)	99.5
Cp(c)−Zr−Im(1)	125.0	Cp(c)−Zr−Im(1)	121.0
Cp(c)−Zr−Im(2)	110.4	Cp(c)−Zr−Im(2)	115.4
N(1)−Zr−Im(1)	101.7	N(1)−Zr−Im(1)	105.6
N(1)−Zr−Im(2)	113.7	N(1)−Zr−Im(2)	111.9
Im(1)−Zr−Im(2)	106.4	Im(1)−Zr−Im(2)	103.1
N(1)−Zr−N(2)	102.61(14)	N(1)−Zr−N(2)	91.26(7)
N(1)−Zr−N(3)	98.03(14)	N(1)−Zr−N(3)	121.13(8)
N(1)−Zr−C(16)	99.7(2)	N(1)−Zr−C(16)	119.96(9)
N(1)−Zr−C(22)	129.8(2)	N(1)−Zr−C(26)	101.34(9)
N(2)−Zr−N(3)	97.1(2)	N(2)−Zr−N(3)	88.53(7)
N(2)−Zr−C(16)	33.3(2)	N(2)−Zr−C(16)	32.52(8)
N(3)−Zr−C(22)	85.1(2)	N(2)−Zr−C(26)	116.62(8)
N(3)−Zr−C(16)	130.0(2)	N(3)−Zr−C(16)	86.29(8)
N(3)−Zr−C(22)	32.1(2)	N(3)−Zr−C(26)	32.90(8)
C(16)−Zr−C(22)	111.0(2)	C(16)−Zr−C(26)	119.17(9)
N(1)−Si−C(1)	96.3(2)	N(1)−Si−C(1)	95.08(11)
Si−N(1)−Zr	104.2(2)	Si−N(1)−Zr	104.48(6)
C(12)−N(1)−Si	124.4(3)	C(12)−N(1)−Si	125.5(2)
C(12)−N(1)−Zr	131.3(3)	C(12)−N(1)−Zr	129.4(2)
C(16)−N(2)−C(18)	128.3(4)	C(16)−N(2)−C(18)	125.0(2)
C(16)−N(2)−Zr	72.6(3)	C(16)−N(2)−Zr	71.23(14)
C(18)−N(2)−Zr	158.5(4)	C(18)−N(2)−Zr	163.8(2)
C(22)−N(3)−C(24)	131.4(4)	C(26)−N(3)−C(28)	128.8(2)
C(22)−N(3)−Zr	71.2(3)	C(26)−N(3)−Zr	72.19(14)
C(24)−N(3)−Zr	157.3(3)	C(28)−N(3)−Zr	158.9(2)
C(5)−C(1)−C(2)	105.1(4)	C(5)−C(1)−C(2)	105.7(2)
C(2)−C(1)−Si	125.5(3)	C(2)−C(1)−Si	121.4(3)
C(5)−C(1)−Si	121.4(4)	C(5)−C(1)−Si	125.6(2)
N(2)−C(16)−C(17)	128.8(5)	N(2)−C(16)−C(17)	122.2(2)
N(2)−C(16)−Zr	74.1(3)	N(2)−C(16)−Zr	76.25(14)
C(17)−C(16)−Zr	156.8(4)	C(17)−C(16)−Zr	161.3(2)
N(3)−C(22)−C(23)	127.7(7)	N(3)−C(26)−C(27)	124.9(2)
N(3)−C(22)−Zr	76.6(3)	N(3)−C(26)−Zr	74.90(14)
C(23)−C(22)−Zr	155.4(3)	C(27)−C(26)−Zr	159.9(2)

[a] Cp(c) is the centroid of the permethylated cyclopentadienyl ring containing atoms C(1), C(2), C(3), C(4), and C(5). [b] Im(1) and Im(2) designate the midpoints of the N(2)−C(16) bond and the N(3)−C bond of the two η^2-iminoacyl ligands, respectively.

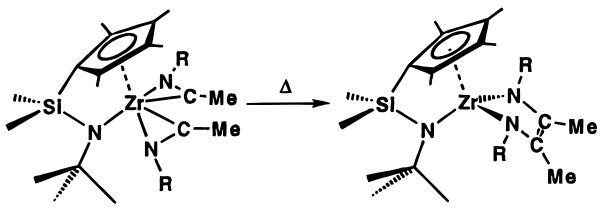

(4)

3 **4**

R = (a) t-butyl; (b) 2,6-xylyl; (c) methyl

were obtained from an evaluation of the temperature dependence of the rate constant in each case. The corresponding rate constants within the temperature range of 70−120 °C are tabulated in Table 1. The activation parameters of $\Delta H^{\ddagger} = 24.6(2)$ kcal/mol and $\Delta S^{\ddagger} = -11.3(7)$ eu for **3a** → **4a** and of $\Delta H^{\ddagger} = 23.9(3)$ kcal/mol and $\Delta S^{\ddagger} = -10.4(8)$ eu for **3b** → **4b** fall within the $\Delta H^{\ddagger}$ range (21.0−25.0 kcal/mol) and $\Delta S^{\ddagger}$ range (−2 to −16 eu) reported by Rothwell and co-workers[16] for the analogous intramolecular C,C-coupling reaction observed for $Zr(OAr)_2[\eta^2\text{-}C(Me)NR]_2$ complexes, where OAr = 2,6-di-*tert*-butylphenoxide and R = *meta*- or *para* substituted phenyl substituent. The negative entropy of activation is consistent with a mechanism that proceeds toward a more symmetric transition state,[16] and the positive enthalpy of activation presumably reflects the collective energy needed to rotate the two η^2-iminoacyl groups toward mutually-similar N-outside orientations as well as weaken the two Zr−C(iminoacyl) bonds.

Table 4. Selected Interatomic Distances (Å) and Bond Angles (deg) for the Zirconium Enediamidate Complexes 4a and 4b[a]

4a		4b	
A. Interatomic Distances			
Zr−Cp(c)	2.244	Zr−Cp(c)	2.211
Zr−N(1)	2.138(4)	Zr−N(1)	2.149(3)
Zr−N(2)	2.068(4)	Zr−N(2)	2.071(3)
Zr−N(3)	2.064(4)	Zr−N(3)	2.069(3)
Zr···C(16)	2.564(5)	Zr···C(16)	2.603(4)
Zr···C(17)	2.563(5)	Zr···C(27)	2.595(4)
Si−C(1)	1.860(5)	Si−C(1)	1.870(4)
Si−N(1)	1.733(4)	Si−N(1)	1.723(3)
N(1)−C(12)	1.501(6)	N(1)−C(12)	1.487(5)
N(2)−C(16)	1.405(6)	N(2)−C(16)	1.413(5)
N(3)−C(17)	1.400(6)	N(3)−C(17)	1.417(5)
N(2)−C(20)	1.491(6)	N(2)−C(20)	1.436(5)
N(3)−C(24)	1.483(6)	N(3)−C(28)	1.423(5)
C(16)−C(17)	1.388(7)	C(16)−C(17)	1.373(5)
B. Bond Angles			
Cp(c)−Zr−N(1)	100.5	Cp(c)−Zr−N(1)	101.5
Cp(c)−Zr−N(2)	123.6	Cp(c)−Zr−N(2)	115.1
Cp(c)−Zr−N(3)	123.3	Cp(c)−Zr−N(3)	116.0
N(1)−Zr−N(2)	110.94(14)	N(1)−Zr−N(2)	120.33(12)
N(1)−Zr−N(3)	113.2(2)	N(1)−Zr−N(3)	119.84(12)
N(2)−Zr−N(3)	85.6(2)	N(2)−Zr−N(3)	84.81(12)
N(1)−Si−C(1)	96.2(2)	N(1)−Si−C(1)	95.9(2)
Si−N(1)−Zr	103.9(2)	Si−N(1)−Zr	103.3(2)
C(12)−N(1)−Si	124.2(3)	C(12)−N(1)−Si	123.3(3)
C(12)−N(1)−Zr	131.9(3)	C(12)−N(1)−Zr	133.4(2)
C(16)−N(2)−C(20)	123.6(4)	C(16)−N(2)−C(20)	120.6(3)
C(16)−N(2)−Zr	93.2(3)	C(16)−N(2)−Zr	94.8(2)
C(20)−N(2)−Zr	141.6(3)	C(20)−N(2)−Zr	142.1(2)
C(17)−N(3)−C(24)	122.1(4)	C(17)−N(3)−C(28)	119.2(3)
C(17)−N(3)−Zr	93.5(3)	C(17)−N(3)−Zr	94.4(2)
C(24)−N(3)−Zr	144.0(3)	C(28)−N(3)−Zr	145.5(3)
C(5)−C(1)−C(2)	105.8(5)	C(5)−C(1)−C(2)	105.6(4)
C(2)−C(1)−Si	122.1(4)	C(2)−C(1)−Si	122.5(3)
C(5)−C(1)−Si	124.5(3)	C(5)−C(1)−Si	124.3(3)
N(2)−C(16)−C(17)	120.4(4)	N(2)−C(16)−C(17)	119.8(3)
N(2)−C(16)−C(18)	119.9(5)	N(2)−C(16)−C(18)	117.7(3)
C(17)−C(16)−C(18)	119.4(5)	C(17)−C(16)−C(18)	122.3(3)
N(3)−C(17)−C(16)	120.4(5)	N(3)−C(17)−C(16)	120.4(3)
N(3)−C(17)−C(19)	120.4(5)	N(3)−C(17)−C(19)	117.7(3)
C(16)−C(17)−C(19)	118.5(5)	C(16)−C(17)−C(19)	121.7(4)

[a] Cp(c) is the centroid of the permethylated cyclopentadienyl ring containing atoms C(1), C(2), C(3), C(4), and C(5).

The NMR spectra for the three enediamidate complexes, **4a**−**c**, are consistent with the presence of a mirror plane of symmetry passing through the bridgehead C, Si, and Zr atoms and bisecting the N−Zr−N angle of the 1,4-diaza-5-zirconacyclopentene ring. Each pair of distal and proximal methyl substituents on the permethylated cyclopentadienyl ring, the two methyl groups of the $SiMe_2$ linkage, and the pair of *cis* methyl

(16) Durfee, L. D.; McMullen, A. K.; Rothwell, I. P. *J. Am. Chem. Soc.* **1988**, *110*, 1463.

groups on the C=C bond exhibit one characteristic ^{1}H and one ^{13}C NMR resonance. As expected, the carbon resonance for the bridgehead carbon[12] of the cyclopentadienyl ring is positioned *ca.* 20 ppm upfield from the corresponding pair of signals for the distal and proximal ring carbons.

The results of our X-ray structural analysis of **4a** and **4b** (vide infra) reveal that their five-membered ZrN_2C_2 rings are significantly folded along the N···N line segment, thereby suggesting the possibility of observing in solution a dynamic equilibrium between two inequivalent folded ring conformations. Rothwell and coworkers[1b] estimated that the activation energy for the corresponding degenerate process in $Zr(OAr')_2$[N(2,6-xylyl)C(Me)=C(Me)N(2,6-xylyl)], where OAr′ is 2,6-di-*tert*-butylphenoxide, is 14.5 (5) kcal/mol at 0 °C. We subsequently found that the activation barrier and coalescence temperature for the analogous process in the related bicyclic enediamidate group 4 metallocene complexes, $(C_5R'_5)_2M[N(R)C(CH_2SiMe_2CH_2)=CN(R)]$, are highly variable and depend on the substituents R and R′ and the metal M.[17] In contrast, upon lowering the temperature of the NMR solutions containing **4a** or **4b**, no noticeable broadening or reduction in the intensities of the ^{1}H NMR resonances was observed, thereby suggesting either that the activation barrier for this interconversion is small (i.e., ≪10 kcal/mol) or that the ring conformations associated with the molecular structures of **4a** and **4b** remain rigid in solution.

Structural Characterization of the Bis(η^2-iminoacyl) Complexes, 3a and 3b. Perspective views of the molecular structures of **3a** and **3b** with the corresponding atom labeling schemes are depicted in Figures 2 and 3, respectively. The pseudotetrahedral coordination spheres about the Zr atoms in these complexes are analogous, consisting of a permethylated cyclopentadienyl ring with an appended t-butylamido ligand and two η^2-bound iminoacyl groups. The angle between the two vectors extending from Zr to the midpoints Im(1) and Im(2) of the two iminoacyl C=N bonds (106.4° (**3a**) and 103.1° (**3b**)) compares well with the Cl−Zr−Cl bond angle of 104.92(4)° in $[(C_5Me_4)SiMe_2(N\text{-t-Bu})]ZrCl_2$.[12] The Zr−N(1) and Cp(c)−Zr distances of 2.184(3) and 2.231 Å in **3a** and of 2.174(2) and 2.236 Å in **3b** are significantly longer than the corresponding distances of 2.052(2) and 2.163 Å in the 14-electron dichloride derivative. Similar elongations of the Zr−N distance and the Zr−Cp(c) separation are observed in $\{[(C_5Me_4)SiMe_2(N\text{-t-Bu})]Zr(\eta^2\text{-}O_2CMe)(\mu\text{-}O_2CMe)\}_2$,[9] which contains a coordinatively saturated ligand environment at each 18-electron Zr(IV) center. By utilizing two additional metal orbitals for bonding, the two 4-electron donating η^2-iminoacyl ligands in **3a** and **3b** reduce the electrophilicity at Zr, thereby diminishing the magnitude of the π-donating interaction of the appended amido functionality. The crowded metal coordination environment in **3a** and **3b** is further accompanied by a modest decrease[12] in the Cp(c)−Zr−N(amido) angle to 99.2° and 99.5°, respectively.

The structural parameters, such as the C=N distance and the internal angles within the three-membered ZrCN rings, are consistent with those reported for other organozirconium compounds containing one,[18] two,[19] or three[19] η^2-iminoacyl ligands. Normally, one finds that

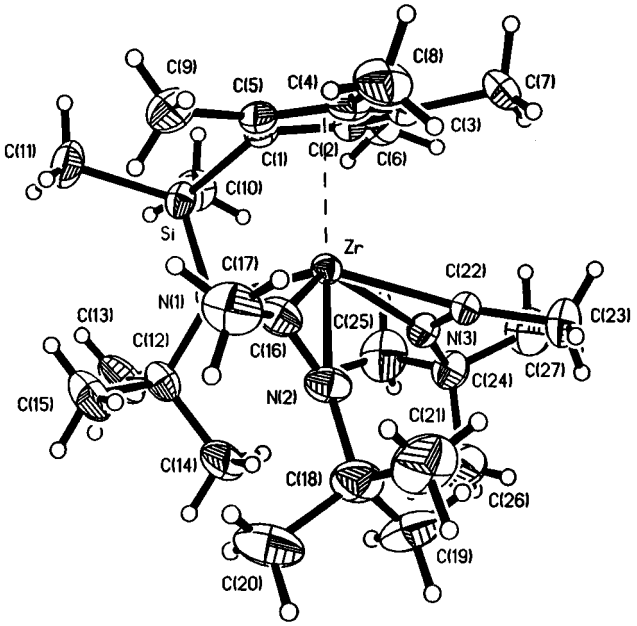

Figure 2. Molecular structure of **3a** with the nonhydrogen atom labeling scheme. The thermal ellipsoids are scaled to enclose 30% probability.

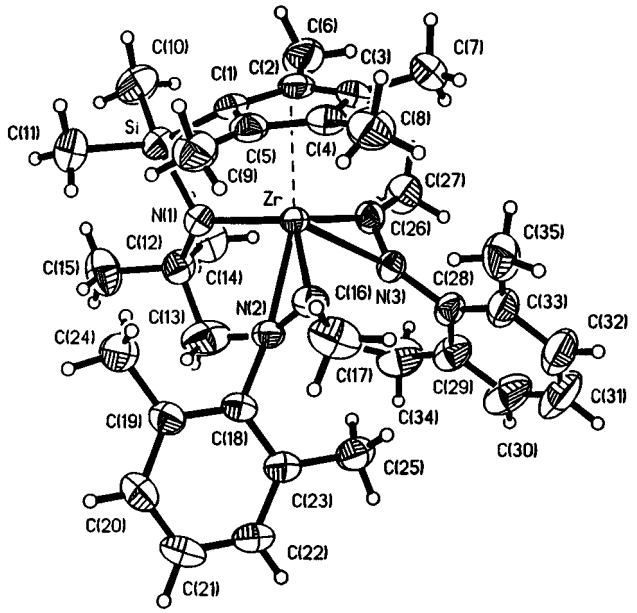

Figure 3. Molecular structure of **3b** with the nonhydrogen atom labeling scheme. The thermal ellipsoids are scaled to enclose 30% probability.

(17) The activation barrier and coalescence temperature for the degenerate interconversion of the five-membered ZrN_2C_2 ring in $(C_5Me_5)_2Zr[N(Me)C(CH_2SiMe_2CH_2)=CN(Me)]$,[2c] $Cp_2Zr[N(CMe_3)C(CH_2SiMe_2CH_2)=CN(CMe_3)]$,[2b] $Cp_2Hf[N(CMe_3)C(CH_2SiMe_2CH_2)=CN(CMe_3)]$,[3a] and $Cp_2Zr[N(2,6\text{-xylyl})C(CH_2SiMe_2CH_2)=CN(CMe_3)]$[2b] are $\Delta G^{\ddagger}$(est.) ≪ 10 kcal/mol, T_c < −110 °C; $\Delta G^{\ddagger}$ = 19.5(5) kcal/mol, T_c = 142 °C; $\Delta G^{\ddagger}$ = 16.9(5) kcal/mol, T_c = 85 °C; and $\Delta G^{\ddagger}$(est.) >> 20 kcal/mol, T_c ≫ 150 °C, respectively.

(18) (a) Reger, D. L.; Tarquini, M. E.; Lebioda, L. *Organometallics* **1983**, *2*, 1763. (b) Erker, G.; Korek, U.; Petersen, J. L. *J. Organomet. Chem.* **1988**, *355*, 121. (c) Bristow, G. S.; Lappert, M. F.; Atwood, J. L.; Hunter, W. E. Unpublished results described in *Chemistry of Organozirconium and Hafnium Compounds*; Cardin, D. F., Lappert, M. F., Raston, C. L., Eds.; Wiley, New York, 1986.

(19) Chamberlain, L. R.; Durfee, L. D.; Fanwick, P. E.; Kobriger, L.; Latesky, S. L.; McMullen, A. K.; Rothwell, I. P.; Folting, K.; Huffman, J. C.; Streib, W. E.; Wang, R. *J. Am. Chem. Soc.* **1987**, *109*, 390.

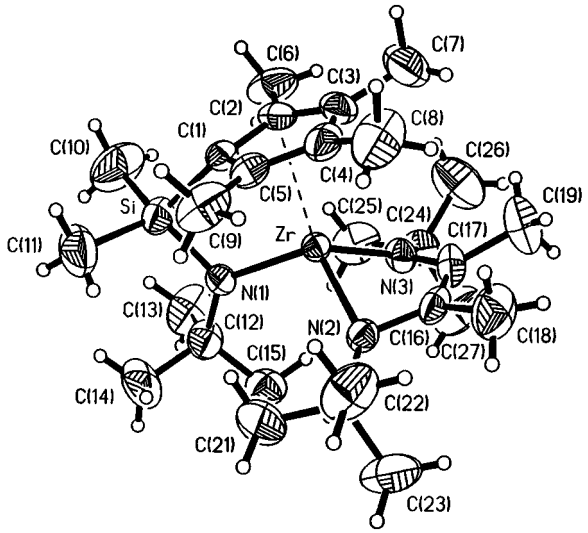

Figure 4. Molecular structure of **4a** with the non-hydrogen atom labeling scheme. The thermal ellipsoids are scaled to enclose 30% probability.

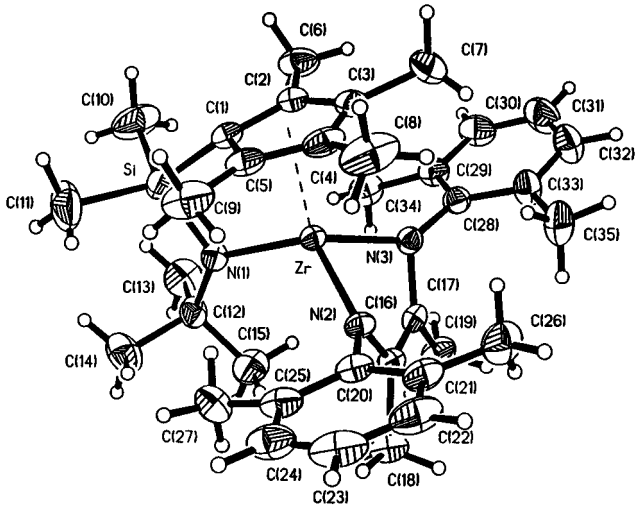

Figure 5. Molecular structure of **4b** with the non-hydrogen atom labeling scheme. The thermal ellipsoids are scaled to enclose 30% probability.

for these Zr η^2-iminoacyl complexes, the Zr−N bond distance is typically equal to or less than the Zr−C bond distance within the same η^2-iminoacyl ligand. However, the opposite trend is observed in **3a** and **3b**. Here, the Zr−N distance in each three-membered ZrCN ring is *ca*. 0.02−0.06 Å longer than the corresponding Zr−C distance. The magnitude of Δd ($d_{Zr-N} - d_{Zr-C}$) correlates directly with the relative orientation of the iminoacyl group with respect to the plane defined by Zr, Im(1), and Im(2). For **3a**, the acute dihedral angles between the planes containing Zr, N(2), C(16) and Zr, N(3), C(22) with the Zr, Im(1), Im(2) plane are 24.3° and 61.1°, respectively, with N(2) and N(3) positioned inside and outside of the wedge defined by the Zr−Im(1) and Zr−Im(2) directions. For **3b**, the acute dihedral angles between the planes containing Zr, N(2), C(16) and Zr, N(3), C(26) with the corresponding Zr, Im(1), Im(2) plane are 90.0° and 14.5°, respectively, with N(3) occupying an inside position. For N(2) in **3a** and N(3) in **3b**, which adopt a nearly N-inside orientation, Δd is 0.017 and 0.031 Å, respectively. In contrast, for the remaining iminoacyl ligand containing N(3) in **3a** and N(2) in **3b**, the respective Δd values of 0.062 and 0.058 Å are considerably larger. The relatively long Zr−N(3) distance of 2.304(4) Å in **3a** and the Zr−N(2) distance of 2.316(2) Å in **3b** probably reflect a poorer orbital match between the available Zr-valence and N-donor orbitals, both of which are directed toward one another from below the Zr, Im(1), Im(2) plane.

Structural Characterization of the Cyclic Enediamidate Complexes, 4a and 4b. The molecular structures of **4a** and **4b** have also been determined by X-ray crystallography, and perspective views of these two enediamidate complexes with their atom labeling schemes are shown in Figures 4 and 5, respectively. The pseudotetrahedral coordination sphere about the Zr atom in both compounds consists of the permethylated cyclopentadienyl ring, the appended amido N, and the two N-donors of a symmetrically-chelating enediamidate ligand generated by the intramolecular C,C-coupling of the two η^2-iminoacyl groups of **3a** and **3b**, respectively. The Zr−N(1) distances of 2.138(4) Å in **4a** and 2.149(3) Å in **4b** correspond to the appended t-butylamido functionality and are substantially longer than the corresponding Zr−N(2) and Zr−N(3) distances which range from 2.06−2.07 Å in **4a** and **4b**. These latter distances are comparable to the Zr−N distances of 2.060(5) and 2.064(4) Å for the terminal dialkylamido ligands in $[(C_5Me_4)SiMe_2(N\text{-}t\text{-}Bu)]Zr(NMe_2)_2$[12] and many other zirconium amido complexes[20] in which an appreciable N π-donation to an electrophilic d^0 Zr center exists. These Zr−N distances for the enediamido ligands of **4a** and **4b** are essentially identical to the values of 2.060(6) and 2.061(6) Å in $Zr(OAr)_2$[N(2,6-xylyl)C(Me)=C(Me)N(2,6-xylyl)][1b] but are noticeably shorter than the Zr−N distances of 2.111(8), 2.104(6) Å in $Cp_2Zr[N(CMe_3)C(CH_2SiMe_2CH_2)=CN(CMe_3)]$;[2b] 2.110(6), 2.112(7) Å in $Cp^*_2Zr[N(Me)C(CH_2SiMe_2CH_2)=CN(Me)]$;[2c] and 2.100(4), 2.123(5) Å in $Cp_2Zr[N(Ph)C(Ph)=C(Ph)N(Ph)]$.[21]

The structural parameters within the 1,4-diaza-5-zirconacylopentene rings of **4a** and **4b** are consistent with a dianionic enediamido ligand donating to a d^0 Zr(IV) center. The C(16)−C(17) bonds of 1.388(7) (**4a**) and 1.373(5) Å (**4b**) fall well within the range 1.35−1.42 Å observed for the C=C double bond in related enamidolate,[1] enediamidate,[1,2,6a] and butadiene complexes[22] that also conform to the metallacyclopentene resonance structure. The N(2)−C(16) and N(3)−C(17) distances of 1.405(6) and 1.400(6) in **4a** and 1.413(5) and 1.417(5) in **4b** are consistent with C−N single bonds.

A notable structural feature associated with the molecular structures of these compounds is the folding

(20) Some representative Zr−N bond distances for Zr(IV) amide complexes: (a) 2.07 Å, $Zr(NMe_2)_4$ (electron diffraction); Hagen, K.; Holwill, C. J.; Rice, D. A.; Runnacles, J. D. *Inorg. Chem.* **1988**, *27*, 2032. (b) 2.06 Å, $(Me_2N)_2Zr(\mu\text{-N-t-Bu})_2Zr(NMe_2)_2$; Nugent, W. A.; Harlow, R. L. *Inorg. Chem.* **1979**, *18*, 2030. (c) 2.06 Å, *rac*-$[C_2H_4(C_9H_6)_2]Zr(NMe_2)_2$; Diamond, G. M.; Jordan, R. F.; Petersen, J. L. *J. Am. Chem. Soc.* **1996**, *118*, 8024. (d) 2.07 Å, *rac*-$[SiMe_2(C_9H_6)_2]Zr(NMe_2)_2$; 2.04 Å, $[\mu\text{-}SiMe_2(C_9H_6)_2]Zr_2(NMe_2)_6$; Christopher, J. N.; Diamond, G. M.; Jordan, R. F.; Petersen, J. L. *Organometallics* **1996**, *15*, 4038. (e) 2.07 Å, $Zr[N(SiMe_3)_2]_3Cl$; 2.08 Å, $Zr[N(SiMe_3)_2]_3Me$; Bradley, D. C.; Chudzynska, H.; Backer-Dirks, J. D. J.; Hursthouse, M. B.; Ibrahim, A. A.; Montevalli, M.; Sullivan, A. C. *Polyhedron* **1990**, *9*, 1423. (f) 2.00 Å, $(C_5Me_5)Zr[N(i\text{-}Pr)_2]Cl_2$; Pupi, R. M.; Coalter, J. N.; Petersen, J. L. *J. Organomet. Chem.* **1995**, *497*, 17.

(21) Scholz, J.; Dlikan, M.; Ströhl, D.; Dietrich, A.; Schumann, H.; Thiele, K.-H. *Chem. Ber.* **1990**, *123*, 2279.

(22) Erker, G.; Krüger, C.; Müller, G. *Adv. Organomet. Chem.* **1985**, *24*, 1 and references cited therein.

of the 1,4-diaza-5-zirconacyclopentene ring along the N···N line segment. For $Zr(OAr)_2[N(R)C(Me)=C(Me)-N(R)]$,[1] $Cp_2Zr[N(Ph)C(Ph)=C(Ph)N(Ph)]$,[21] and $Cp_2Zr-[N(R)C(CH_2SiMe_2CH_2)=CN(R)]$,[2] the two possible folded conformations represent degenerate structures, and thus only one conformational structure is observed in the solid state. In contrast, the presence of the bifunctional *ansa*-monocyclopentadienylamido ligand in **4a** and **4b** offers the possibility of observing two inequivalent conformations for the folded 1,4-diaza-5-zirconacyclopentene ring. If we adopt the analogous nomenclature recently used to define the conformational geometry of the coordinated diene in $[(C_5Me_4)SiMe_2(N\text{-}t\text{-}Bu)]Ti(diene)$ complexes,[23] then the ring conformer with the 1,4-diaza-5-zirconacyclopentene ring folded up toward the cyclopentadienyl ring corresponds to the prone structure because the open end of the cup defined by atoms N(2), C(16), C(17), and N(3) is oriented away from the cyclopentadienyl ring. The other ring conformer corresponds to the supine structure because the opening of the cup is directed toward the cyclopentadienyl ring. On the basis of this nomenclature, the 1,4-diaza-5-zirconacyclopentene ring of **4a** exhibits the prone structure with the acute dihedral angle between the planes containing Zr, N(2), N(3) and N(2), C(16), C(17), N(3) being 50.5° and the corresponding five-membered ring of **4b** adopts the alternative supine structure with the dihedral angle being 49.0°. Given that these folding angles are comparable in magnitude, one might expect that the prone structure should be sterically less favorable. However, the dihedral angle between the plane of the cyclopentadienyl ring and the plane containing Zr, N(2), N(3) of 53.0° for the prone structure is *ca.* 12° greater than the corresponding dihedral angle of 41.1° associated with the supine structure of **4b**. This structural alteration apparently compensates for the steric interactions imposed by the prone conformation.

In both **4a** and **4b**, ring folding moves the internal carbons, C(16) and C(17), of the 1,4-diaza-5-zirconacyclopentene ring closer to the electrophilic Zr center. The corresponding Zr−C(16) and Zr−C(17) distances of 2.564(5) and 2.563(5) Å in **4a** and 2.603(4) and 2.595(4) Å in **4b** imply that both conformers could experience some stabilization from a weak attractive interaction between the filled π-orbital of the C=C double bond and an empty metal orbital that is directed above and below the Zr, N(2), N(3) plane. However, the absence of any significant elongation or notable difference in the C(16)−C(17) bond distances in **4a** and **4b** suggests that this type of π-interaction is probably not a major factor in determining the relative stability and conformational preference of the nonplanar prone and supine structures in **4a** and **4b**, respectively.

The bending of these five-membered rings is more likely a consequence of the presence of the *tert*-butyl or 2,6-xylyl substituent at each N atom of the enediamido ligand. Folding along the N(2)···N(3) line segment (in either direction) enhances the overlap of the p_π-orbital at each N with the same laterally disposed vacant metal orbital and thus helps account for the observed reduction in the Zr−N(2) and Zr−N(3) distances mentioned earlier. However, because the magnitude of the ring folding is comparable for **4a** and **4b**, the degree of π-stabilization associated with these Zr−N bonds is expected to be similar and, thus, explains why the Zr−N distances are essentially equal for the prone and supine conformations.

In view of the similar electronic features displayed by these folded metallacylic rings, why do the 1,4-diaza-5-zirconacyclopentene rings of **4a** and **4b** adopt different conformational structures? The explanation apparently lies in considering the steric features imposed by the different size and shape of the substituents at N(2) and N(3) of the folded ZrN_2C_2 rings. In **4a**, the prone structure directs the bulky *tert*-butyl substituents away from the methyl substituents at C(2) and C(5) of the cyclopentadienyl ring. In contrast, the supine structure of **4b** allows both planar 2,6-xylyl groups to lie parallel to the plane of the cyclopentadienyl ring. By minimizing the steric interactions between the methyl substituents of the 2,6-xylyl and cyclopentadienyl rings, this arrangement reinforces the structural preference for the supine conformation observed for **4b**.

Acknowledgment. Financial support for this research was provided by the National Science Foundation (Grant No. CHE-9113097). J.L.P. gratefully acknowledges the support provided by the Chemical Instrumentation Program of the National Science Foundation (Grant No. CHE 9120098) to acquire a Siemens P4 X-ray diffractometer in the Department of Chemistry at West Virginia University.

Supporting Information Available: Tables of crystal data and structure refinement, atomic coordinates, interatomic distances and bond angles, anisotropic displacement parameters, and hydrogen coordinates for **3a**, **3b**, **4a**, and **4b** (29 pages). Ordering information is given on any current masthead page. Structure factor tables for these four compounds are available from the authors upon written request.

OM9610760

(23) Devore, D. D.; Timmers, F. J.; Hasha, D. L.; Rosen, R. K.; Marks, T. J.; Deck, P. A.; Stern, C. L. *Organometallics* **1995**, *14*, 3132.